

# Characterization, destruction and recycling of pure asbestos and asbestos containing waste (ACW)

Talbi G.<sup>1</sup>, Cambon M.<sup>1</sup>, Nonat A.<sup>2</sup> And Cambon O.<sup>1,\*</sup>

<sup>1</sup>Institut Charles Gerhardt Montpellier, Centre National de la Recherche Scientifique, Université de Montpellier, Ecole Nationale Supérieure de Chimie de Montpellier, Montpellier 34095, Cedex 5, France.

<sup>2</sup>Laboratoire interdisciplinaire Carnot de Bourgogne, UMR 6303 CNRS-Université de Bourgogne, 9 Av. A. Savary, BP 47870, F-21078 Dijon Cedex, France.

\*corresponding author: O. Cambon

e-mail: olivier.cambon@umontpellier.fr

## Abstract

In the current context, the treatment of industrial waste is an essential economic and environmental issue. At this time, considering the safety standards which banish asbestos from the environment, the stocks of asbestos containing waste are considerable and their elimination is a major problem. This work is based on the development of new processes of destructions termed "green" to replace the plasma process, which is used today and which presents a prohibitive energy and economic cost. Various techniques (SEM-EDX, XRD, NMR, IR-ARO and TEM) were used to characterize pure asbestos and ACW. XRD is the most efficient technique to distinguish the different kinds of asbestos like chrysotile and amphiboles. Based on these results, an acid treatment is applied allowing to dissolve the cement matrix and to transform the chrysotile. In the case of chrysotile containing waste, the solid obtained is pure silica which is then used to synthesize a nitrate-cancrinite. In the case of the presence of amphiboles in the starting ACW, a treatment in a basic environment is applied under hydrothermal conditions leading to entirely dissolve the waste.

**Keywords:** Asbestos, destruction, recycling, process, nitrate-cancrinite.

## 1. Introduction

Asbestos is a series of natural fibers known for more than 2000 years, it began to be mass-produced in 1877 in Quebec. During the last century, millions of tons of fibers were extracted and used in many fields such as the construction or textile industry. The use of asbestos is due to its interesting properties, for instance: fire and chemical resistance. The most recent common application is asbestos-cement which represents 95% of the use of asbestos: all these materials are called asbestos containing material (ACM) [1]. It is well known for a very long time that asbestos is very harmful for the human body but it is only during the period from 1980-1990 that its use was forbidden in many countries. Indeed, the physicochemical characteristics of asbestos, and its ability to be cut into microscopic particles enable it to reach pulmonary alveoli. Thus inhalation of fibers particles is dangerous (it can cause cancer such as pleural mesothelioma) [2]. Because of its

ban, asbestos is going to generate millions of ton of waste (asbestos containing waste, ACW). These wastes must be neutralized and transformed via an economical process. Serpentine and amphiboles are the two mineralogical groups of asbestos. The Serpentine group contains only one variety: chrysotile (or white asbestos), with chemical formula  $[3\text{MgO} \cdot 2\text{SiO}_2 \cdot 2\text{H}_2\text{O}]$ , which is the most important commercial source of asbestos (95% of the market). Chrysotile is a layered silicate: the first layer is composed of  $\text{SiO}_4$  tetrahedra and the second is a  $\text{MgO}_6$  octahedra layer [3]. Due to the difference of the size between  $\text{MgO}_6$  and  $\text{SiO}_4$  polyhedra, the octahedra layer induces a general bending of the structure giving a tube shape to the chrysotile, the  $\text{MgO}_6$  layer being the external one [4]. The amphibole group is composed of five varieties of asbestos: amosite/grunerite (or brown asbestos), crocidolite (or blue asbestos), tremolite, actinolite and anthophyllite. The amphibole structure is a series of double chains ( $\text{Si}_4\text{O}_{11}$ ) parallels to the c axis. The layers of  $\text{MO}_6$  octahedra (with  $\text{M} = \text{Mg, Fe, Na}$ ) are stacked between both layers of  $\text{SiO}_2$  [5]. The difference of structure between serpentine and amphiboles is thus going to have an important role in the chemical sensitivity towards the solvent used. Previous studies have been already published on chrysotile asbestos destruction using an oxalic acid based treatment [6]. In the present work, different types of asbestos (Serpentine and amphiboles) and ACW were collected and characterized by using different techniques. In a second step the different wastes were destroyed by using acid and basic solutions under hydrothermal conditions. Finally, a recycling process of the silica obtained after the acid treatment is proposed to synthesize a zeolite.

## 2. Experimental

### 2.1. Samples

Three types of pure asbestos (chrysotile, amosite and crocidolite) and two types of ACW were studied. The two types of ACW are asbestos-cement: the first sample is a roof-tile and the second is a seal used water pipes.

### 2.2. Instrumentation

Samples were analyzed by x-ray powder diffraction (XRD) measurements performed on a BRUCKER D2 phaser x-ray

diffractometer using a Ni-filtered Cu  $\alpha$  radiation ( $\lambda=1.54\text{\AA}$ ) with a step of  $0.014^\circ$  in  $2\theta$ . Scanning Electron Microscopy (SEM) was realized by using a FEI Quanta 200 FEG kitted out by a low- vacuum SED (LFD) detector. The acceleration voltage was about 15kV. This analysis method was coupled with Energy Dispersive X-ray (EDX). Fourier transform infrared spectroscopy in all reflecting object mode (FTIR-ARO) spectra of the samples were acquired in the mid-infrared range ( $4000\text{-}650\text{cm}^{-1}$ ) using an Horiba Jobin Yvon – LabRAM ARAMIS spectrometer equipped with a liquid nitrogen cooler MCT detector. X-ray fluorescence (XRF) analysis were performed by using a Panalytical Epsilon 3<sup>X</sup> spectrophotometer equipped with an Ag-tube (30kV and 3mA) and different filters (Ag, Al and Ti). Solid-state  $^{29}\text{Si}$  Nuclear Magnetic Resonance (NMR) spectra were acquired on a Varian 400 MHz spectrometer. The relaxation delay  $d_1$  between accumulations was 5s. Transmission Electron Microscopy (TEM) analyses were performed on a JEOL 2200FS microscope operated at 200 kV. This microscope is equipped with a field emission gun (FEG) and an in-column Omega-type energy filter. To avoid long electron beam exposure, all microscope and beam adjustments were performed on a sacrificial part of the sample, and images were obtained with the minimum electron dose. Before observations, the samples were directly deposited on a carbon film copper grid. Some specimens were placed in flat embedding molds in fresh LR white resin, and left at  $37^\circ\text{C}$  for slow polymerization and then were cut with a diamond knife (Diatome) in ultrathin sections (80 nm) and placed on carbon coated copper grids.  $\text{N}_2$  adsorption-desorption isotherms at 77 K were recorded with a Micromeritics Tristar analyzer and the specific surface area of the samples was determined using the Brunauer Emmett Teller (BET) method. Before the measurements, the samples ( $\approx 188$  mg) were degassed at  $120^\circ\text{C}$  during 12h under reduced pressure. The destruction of the asbestos and the ACW was performed in two steps. During the first step the samples were treated with nitric acid solutions (2 or 4M) in a 1L reactor while stirring, heated to a temperature of  $80^\circ\text{C}$ . During the second step, the samples were dissolved in NaOH (7M to 10M) under hydrothermal conditions by using a PTFE-lined autoclave (50 mL) heated at  $180^\circ\text{C}$ .

### 3. Results and discussion

#### 3.1. Characterization

The various type of asbestos (amphiboles and serpentine) and ACW were analyzed with SEM (Fig1) and EDX (Table1) to determine their morphology and their chemical composition. The amphiboles appear to be rigid sticks/fibers whereas chrysotile fibers seem to be much more flexible. EDX analysis of the pure asbestos confirms the chemical formula of the different types of asbestos. [6]. EDX analyses of the fibers confirm the previous SEM observations. As it is shown in Table 1, the EDX analyses of different fibers provide information about the nature of the fibers included in both wastes. The Mg/Si ratio measured in the only type of fiber found in the roof tile is 1.26, which is almost equal to the Mg/Si ratio of chrysotile (1.27). It is the same for the flexible fiber observed in the seal of the pipe with a Mg/Si ratio of 1.25. Regarding the other type of fiber in the seal, the results are more

complicated to interpret because the presence of sodium indicates that these fibers could be crocidolite.

As shown in Figure 1, the pipe seal type waste seems to present two types of fibers with different aspects: flexible fibers (a) and rigid fibers (b) which would end to the assumption that there are two types of asbestos. Concerning the roof tile; only the flexible fiber is observed (c).

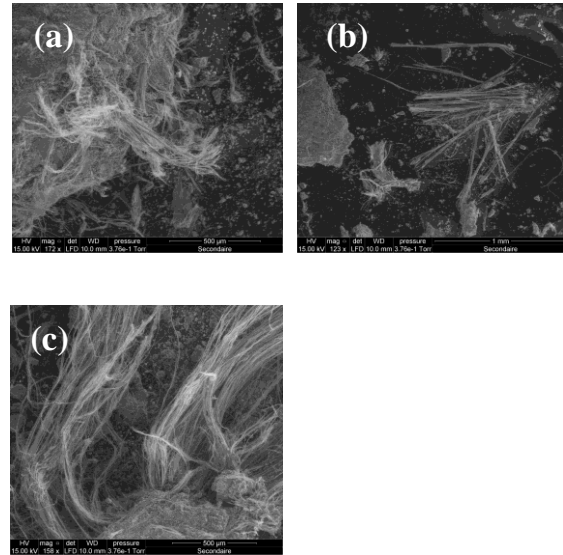


**Figure 1.** SEM photographs of ACW

- (a) Flexible fibers in pipe seal ACW
- (b) Rigid fibers in pipe seal ACW
- (c) Fibers in roof tile ACW

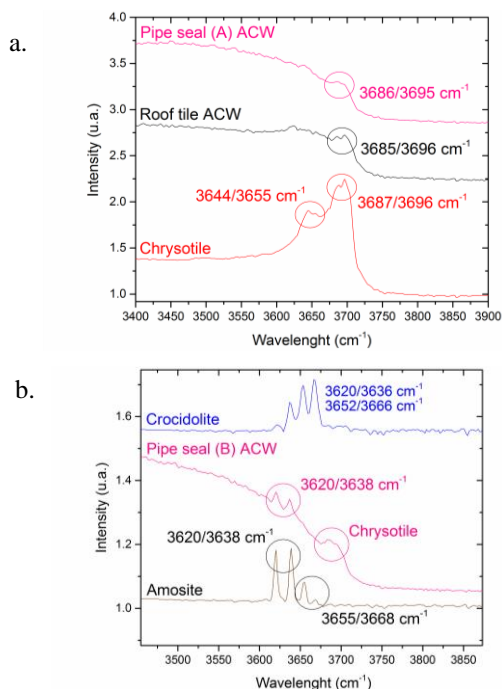
However the Fe/Si ratio indicates that those fibers are mostly fibers of amosite (Fe/Si ratio: fibers = 0.63, crocidolite = 0.26, amosite = 0.63). EDX does not allow to determine, in this case, which of these two amphibole are present in the pipe seal. To conclude for SEM-EDX analysis, the presence of chrysotile is clearly highlighted in both wastes, but it remains to be determined the nature of the second type of fiber present in the pipe seal (crocidolite or amosite). OH vibration modes of asbestos were measured by infrared spectroscopy in the  $3700\text{-}3600\text{cm}^{-1}$  region (Figure 2) corresponding to the absorption due to the stretching mode of the OH groups in the silicate. Analysis of the IR spectrum revealed the presence of characteristic peaks for each type of asbestos [7, 8]. FTIR-ARO spectroscopy can be therefore proposed as an analytical technique to determine the different phases of asbestos in an ACW. As it was demonstrated, the infrared spectrum (figure 2.a) confirms the presence of chrysotile in both ACW. The characteristic peaks of chrysotile are also found in the fiber, which was supposed to be an amphibole (figure 2.b). This is due to the difficulty to isolate the amphibole fibers. In this case, the two types of fibers are overlapped. So, both fibers are analyzed together. On the spectrum of the pipe seal: two peaks appear at  $3620$  and  $3638\text{cm}^{-1}$ . These two peaks may correspond to amosite and crocidolite (see part on pure asbestos), but by comparing the intensities of pure asbestos peaks with those on the spectrum of the pipe seal, it seems that these fibers are mostly of amosite type. Further investigations are

**Table 1.** Chemical composition (mole percent) determined by EDX on pure asbestos and ACW.

Sample	Emp. formula	(%)O	(%)Na	(%)Mg	(%)Si	(%)Fe	%(Ca)
Roof tile a	-	62(1)	-	19.1(3)	15.2(8)	0.8(1)	2.8(2)
Pipe seal b	-	66.3(9)	-	14.9(3)	11.9(7)	0.6(1)	6.3(3)
Pipe seal c	-	62(2)	3.8(1)	3.1(2)	17.1(4)	10.8(6)	2.8(4)
Chrysotile	H <sub>4</sub> Mg <sub>3</sub> O <sub>9</sub> Si <sub>2</sub>	57(1)	-	23.2(4)	18.3(7)	0.7(1)	0.4(2)
Amosite	Fe <sub>11</sub> H <sub>4</sub> Mg <sub>3</sub> O <sub>48</sub> Si <sub>16</sub>	65(2)	-	4.1(2)	19(1)	12.1(7)	-
Crocidolite	Fe <sub>2</sub> H <sub>2</sub> Mg <sub>3</sub> Na <sub>2</sub> O <sub>24</sub> Si <sub>8</sub>	62(1)	4.6(2)	6.9(1)	21.2(5)	5.5(9)	-

such as amosite and crocidolite. In the roof tile and pipe seal ACW, the cement matrix peaks are indexed as calcite

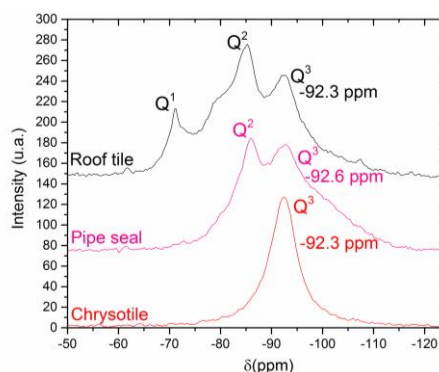
(CaCO<sub>3</sub>) phases. There are also traces of ettringite (Ca<sub>6</sub>Al<sub>2</sub>(SO<sub>4</sub>)<sub>3</sub>(OH)<sub>12</sub>·26H<sub>2</sub>O) in the waste.

**Figure 2.** FTIR-ARO spectra of pure asbestos and ACW

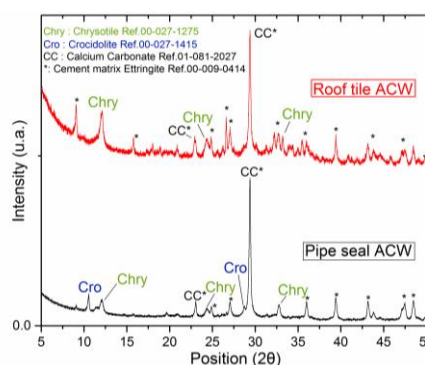
a. IR spectra of chrysotile

b. IR spectra of amphibole

necessary. Solid-state <sup>29</sup>Si NMR analysis was performed to confirm the presence of chrysotile in the two ACW. Figure 3 demonstrates that the chrysotile is present in both types of waste. Indeed, the peak corresponding to the Q<sup>3</sup> line of the silicon appears in the spectra at the same position (approximately -92.3 ppm). The presence of different silicon peaks (Q<sup>1</sup> and Q<sup>2</sup>) in the NMR spectra are due to the presence of silicon atoms with a different chemical environments in the cement matrix of this waste. The amphibole spectra cannot be compared with those of the ACW because they did not give a signal due to the presence of iron in the ACW. Because of its magnetism, iron prevents the NMR activity of silicon. The pattern of the roof tile waste presents only the characteristic peaks from chrysotile (12.05 and 24.30°) whereas the pattern of the pipe seal waste presents the characteristic peaks of chrysotile and crocidolite (28.76°) but no peak of amosite (27.25°). Thus the XRD method allows to clearly identify the various types of asbestos present in ACW: this technique even allows to differentiate similar amphiboles

**Figure 3.** Solid <sup>29</sup>Si NMR of ACW and chrysotile

Powder XRD was used for identifying the different kinds of asbestos in the ACW (figure 4).

**Figure 4.** x-ray diffracting patterns of roof tile and pipe seal ACW

### 3.2. Destruction

#### 3.2.1 Acid treatment

Both types of ACW were treated separately with nitric acid for 7 days. After treatment a gel in suspension was separated by filtration and a solid “block” was recovered in the bottom of the reactor. The mass loss is about 90% of the initial mass of the samples. All parts (solutions, gel and the block) recovered after treatment were analyzed by using XRF to establish a mass balance (Table 2). The

solids (gel and block) were also characterized by using powder XRD, BET, TEM and IR spectroscopy.

**Table 2.** XRF results after acids treatments.

Samples	%Mg	%Al	%Si	%Ca	%Fe
Roof tile	15	8	34	37	5
Roof tile sol.	2	22	0	65	12
Roof tile gel	0	0	>98	0	0
Roof tile block	0	0	>98	0	0
Pipe seal	10	6	25	52	8
Pipe seal sol.	1	18	0	68	13
Pipe seal block	1	0	93	0	6

The solutions recovered after acid treatment mostly contain calcium as well as iron, magnesium and aluminum (Table 2). The cement matrix was therefore dissolved. From the initial waste, silicon is the only element which is not dissolved. It is recovered in the gel and in the block in the bottom of the reactor. For the tile ACW chemical analysis demonstrates that cement matrix is dissolved and the chrysotile is transformed. For the pipe-seal ACW, the chemical composition of the solution is similar to that obtained after the acid treatment of the tile ACW, but in the solid block resulting from the dissolution of the pipe-seal, some iron remains and also with some magnesium which indicates that the amphibole (crocidolite) was not dissolved by the acid treatment. After acid treatment no characteristic peak of the chrysotile was found in the waste after treatment of the roof tile (Figure 5). As for the pipe seal treatment, all the characteristic peaks of crocidolite are found. This demonstrates that the acid treatment eliminates serpentine-type asbestos, but not amphibole-type asbestos. It will therefore be necessary to carry out a second treatment to completely destroy the ACW (see section 3.2.2). The roof tile gel was analyzed in  $N_2$  adsorption-desorption. The surface area measured by using BET method is of  $114.98 \text{ m}^2/\text{g}$  with a pore volume of  $0.260 \text{ cm}^3/\text{g}$  and an average pore size of  $97.3 \text{ \AA}$ .

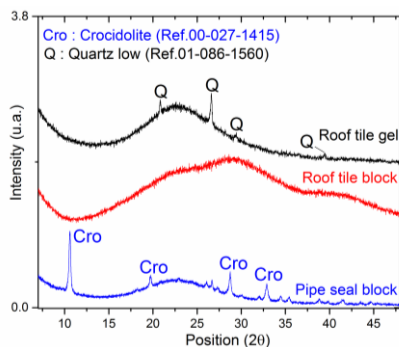


**Figure 5.** X-ray diffracting patterns of the solids after acid treatment

Roof tiles ACW before and after acid treatment were characterized by using IR spectroscopy (Figure 6). As seen previously the spectrum of the ACW presents the characteristic double peak of chrysotile. The double peak at  $2850$  and  $2920 \text{ cm}^{-1}$  is due to the symmetrical and

asymmetric  $\text{CH}_2/\text{CH}_3$  vibration modes from trace organics in the cement matrix [9]. In the spectrum of the gel, the peaks the chrysotile have disappeared which confirms that the treatment with acid completely transforms the chrysotile.

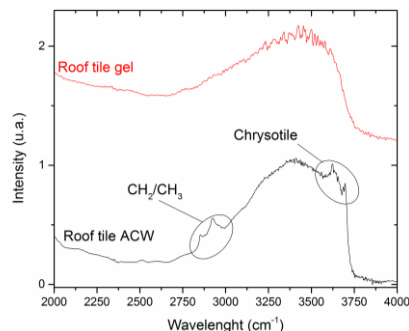


**Figure 6.** FTIR ARO spectra of roof tile ACW before and after acid treatment.

However, in figure 7, the TEM images demonstrate that the fibers are always present in the gel. Moreover, a chemical analysis carried out by transmission on these fibers showed that this fibers are composed of more than 99% of silica.

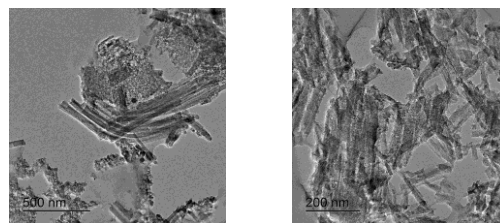


**Figure 7.** TEM photographs of roof tile after acid treatment.

Thus, the acid treatment eliminates the magnesium part of the fibers (the layer of brucite  $\text{Mg}(\text{OH})_2$ ) from the fibers of chrysotile. The dissolution of the brucite layer is due to the chrysotile structure, which leaves the brucite layer accessible in the acid solvent. However these silica fibers have the same length as the chrysotile fibers suggesting that they could be still dangerous. However the acid process does not destroy amphiboles because in their structures, the soluble layer of  $\text{MO}_6$  octahedra is confined between two  $\text{SiO}_2$  layers insoluble in acid solvent. In part 3.3 of this paper, a recycling process is proposed for reusing this mesoporous fibrous silica for synthesizing another material.

### 3.2.2 Alkaline treatment

The dissolution tests in alkaline solutions under hydrothermal conditions were carried out on several types of samples of amphiboles: pure crocidolite, pure amosite and on ACW pipe seal which was previously treated with the nitric acid. The treatment was carried out for 5 days. The solutions obtained after treatment were analyzed by using XRF spectroscopy (Table 3). After alkaline treatment all the waste is completely dissolved, the silicon is recovered in solution. A suspension of iron was found in the solution, which would explain the presence of iron (1%) in the XRF analyses. In conclusion, the alkaline process completely destroys amphibole type asbestos.

**Table 3.** Chemical composition of the solutions after alkaline treatments

Samples	Na	Mg	Si	Fe
Crocidolite Sol.	82%	1%	15%	1%
Amosite Sol.	83%	0%	16%	1%
Pipe seal Sol.	81%	0%	18%	1%

### 3.3 Recycling

The silica obtained after acid treatment of ACW was used to synthesize a nitrate-cancrinite with the chemical formula  $\text{Na}_8[\text{Al}_6\text{Si}_6\text{O}_{24}](\text{NO}_3)_2 \cdot 4\text{H}_2\text{O}$ . The structure of this zeolite consists of small cages ( $\epsilon$ -cages) which form a chain [10].

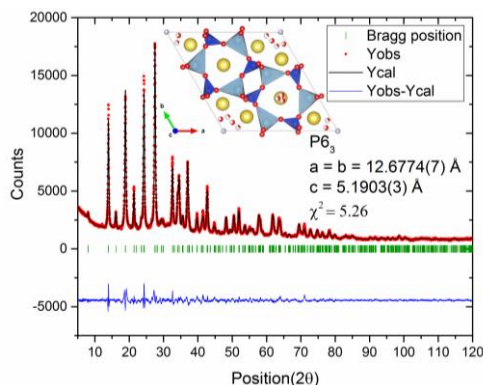


**Figure 8.** X-ray diffracting patterns of nitrate-cancrinite synthesized

Nitrate-cancrinite is used for its adsorption properties. This zeolite has many applications in numerous domains like in pharmaceutical applications [11]. This synthesis of nitrate-cancrinite is inspired by that described by Liu and al [12]. The structure was refined by a Rietveld model using the structure of Fechtelkord *et al.* [13] as the starting model. This synthesis demonstrates that it is possible to reuse the waste following the previous chemical treatments of the ACW.

## 4. Conclusion

Numerous physico-chemical techniques of characterization have been used to identify the asbestos. XRD is the most powerful technique to differentiate the different kinds of asbestos in the ACW (chrysotile, amosite and crocidolite). A chemical process was studied to neutralize and transform the asbestos containing waste. First, nitric acid is used to dissolve the cement matrix and transform the chrysotile. For the chrysotile containing waste a mesoporous silica is obtained which is usable to synthesize a zeolite (nitrate-cancrinite). For the amphibole containing waste a second alkaline treatment must be performed to completely destroy the amphibole type asbestos.

## Acknowledgment

The authors thank Nîmes Métropole for the financial support, IUT of Nîmes and the ANAMAT (ANALYSIS of MATERIALS). The authors are very grateful to J.Haines and M.Poienar for very fruitful discussions. The authors would like also to thank the National Museum of Natural History of Paris and C. Ferraris for providing pure asbestos and finally the SOMEZ Company for the ACW samples.

## References

- IRoss, M. and R.L. Virta, Canadian Mineralogist, 2001: p. 79-88.
- Ladou, J., *et al.*, Environmental Health Perspectives, 2010. **118**(7): p. 897-901.
- Yada, K., Acta Crystallographica, 1967. **23**: p. 704-&.
- Yada, K., Acta Crystallographica Section a-Crystal Physics Diffraction Theoretical and General Crystallography, 1971. **A 27**(NOV1): p. 659-&.
- Warren, B.E., Zeitschrift Fur Kristallographie, 1930. **72**(5/6): p. 493-517.
- Valouma, A., *et al.*, Journal of Hazardous Materials, 2016. **305**: p. 164-170.
- Edwards, H., Journal of Applied Chemistry, 1970. **20**(3): p. 76-+.
- Patterson, J.H. and D.J. Oconnor, Australian Journal of Chemistry, 1966. **19**(7): p. 1155-+.
- Gomes, C.E.M., O.P. Ferreira, and M.R. Fernandes, Materials Research, 2005. **8**: p. 51-56.
- Barrer, R.M. and J.F. Cole, Journal of the Chemical Society a - Inorganic Physical Theoretical, 1970(9): p. 1516-&.
- Linares, C.F., *et al.*, Microporous and Mesoporous Materials, 2005. **77**(2-3): p. 215-221.
- Liu, Q.Y., H.W. Xu, and A. Navrotsky, Microporous and Mesoporous Materials, 2005. **87**(2): p. 146-152.
- Fechteldkord, M., F. Stief, and J.C. Buhl, American Mineralogist, 2001. **86**(1-2): p. 165-175.